Continuity with respect to the speed for optimal ship forms based on Michell's formula

Julien Dambrine, Morgan Pierre

CONTINUITY WITH RESPECT TO THE SPEED FOR OPTIMAL SHIP FORMS BASED ON MICHELL'S FORMULA

JULIEN DAMBRINE AND MORGAN PIERRE

Abstract. We consider a ship hull design problem based on Michell's wave resistance. The half hull is represented by a nonnegative function and we seek the function whose support has a given area and which minimizes the total resistance for a given speed and a given displacement. We show that the optimal domain depends only on two parameters without dimension, the viscous drag coefficient and the Froude number of the area of the support. We prove that the optimal hull depends continuously on the Froude number and that the contribution of Michell's wave resistance vanishes as the Froude number tends to infinity. Numerical simulations confirm the theoretical results for large Froude numbers. For Froude numbers typically smaller than 1, the famous bulbous bow is numerically recovered. For intermediate Froude numbers, a "sinking" phenomenon occurs. It can be related to the nonexistence of a minimizer.

1. Introduction

In this paper, we are interested in finding ship hulls which minimize the resistance of water to the motion of a ship. We focus on a model which involves Michell's wave resistance formula [30], in which the ship moves at constant speed in calm water. The total resistance is the sum of the wave resistance and of the viscous resistance. The viscous resistance is computed in a standard way: it is proportionnal to the square of the speed of the ship and to the area of the wetted hull (see, e.g., [3, (2.19)-(2.21)]).

Finding a hull which minimizes this total resistance, for a given displacement and a given velocity of the ship, is a problem which has been extensively studied. Michell's theory is a first order model in which the hull is assumed to be similar to a vertical plate: this is known as the *thin ship* assumption [25, 30, 31]. A similar expansion on the area functional yields the Dirichlet energy. Thus, the optimal design problem consists in minimizing a quadratic functional (the total resistance) under a linear constraint (the given displacement).

Krein and Sisov [26, 32] proved that this problem is well-posed. By solving a linear integro-differential equation, they showed that a unique solution exists in the class of continuous functions. Closely related problems involving Michell's formula were also studied numerically, theoretically and experimentally by several authors (see [14, 17, 24, 27, 28, 29] and [36, p. 209]). It is also natural to require for the hull to be represented by a nonnegative function [26], in order to avoid self-crossing. In such a case, the constraint is no longer a linear equality, but a set of linear

Laboratoire de Mathématiques et Applications, Université de Poitiers, CNRS, F-86073 Poitiers, France.

This works benefited from the support of the project OFHYS of the CNRS 80|prime 2019 initiative.

inequalities. The problem which was previously linear falls now into the range of quadratic programming [14, 17, 24, 27].

The numerical simulations in [14, 24, 27] showed that the famous *bulbous bow* [15, 20] can be very efficient in minimizing the total resistance, for some values of the parameters. In some cases, a midship bulb was also found to be interesting [11, 17, 23, 24].

In the discussion above, the domain of arguments was *fixed*. Mathematically speaking, the domain of arguments is the support of the hull function. Physically, it is the longitudinal cross-section of the wetted hull. In [13], the authors proposed to consider the domain of arguments as the unknown of the problem. The area of the support was kept fixed in order to be consistent with the thin ship assumption. This geometric shape optimization approach [1, 8, 22] allows to minimize even more the total resistance. In [13], an optimal domain was proved to exist and a bulbous bow was numerically obtained. It was also proved that Michell's wave resistance kernal belongs to $L^{5/4-\varepsilon}$ and that consequently, the optimal hull was locally Hölder continuous.

Our purpose in this paper is to understand how the optimal domain depends on the speed of the ship, whithin the framework of [13]. We first introduce a nondimensional version of the problem, which shows that the optimal domain depends only on a *area Froude number*, once the viscous drag coefficient is set (Section 2). The behaviour of the Dirichlet energy and of the wave resistance functional are analyzed separately in Section 3.

In Section 4, we show that the optimal hull depends continuously on the Froude number. For this result, the Γ-convergence of the functionals in H^1 is first established. We note that the Sobolev space H^1 is associated to the Dirichlet energy in a natural way. Similarly, we show by means of Γ-convergence that the contribution of Michell's wave resistance becomes negligeable as the Froude number tends to $+\infty$.

We explain our numerical approach in Section 5. In particular, we use the Froude invariance to recover normalized domains. In Section 6, we present the optimal domains obtained numerically for a large variety of Froude numbers. Three types of regimes are identified. For small to moderate (area) Froude numbers, typically between 0.5 and 1, the optimal domain exhibits a bulbous bow. For large Froude numbers, the viscous resistance is dominant in the model and the domain ressembles a half disc, as predicted by the theory. For intermediate Froude numbers, the domain is driven far beneath the free surface by the minimization algorithm. This "sinking" process can be related to the non-existence of a minimizer in the case where no bounding box is added to the formulation of the problem. It gives a new interpretation to the midship bulbs obtained by some authors in the case of a fixed domain [18, 23, 24].

Our results for a variable domain give a new insight into the past approaches of the problem for a fixed domain. The total resistance of a ship based on Michell's formula and on the Dirichlet energy is a model which appears frequently in the literature. We confirm that it can be used as a toy model in the spririt of the Newton problem of optimal profiles [9, 10]. Michell's wave resistance alone has an importance which has been underlined in the past decades [19, 33, 34, 35]. Contemporary studies show that it can still prove fruitful in ship hull optimization [2, 4, 17].

2. Formulation of the shape optimization problem

2.1. **Functional setting.** Let D be a nonempty open subset of $\mathbb{R}^2$. The standard Sobolev space $H^1(D)$ is equipped with the Hilbertian norm $\|u\|_{H^1}^2 = \int_D u^2 + \int_D |\nabla u|^2$. We denote $H_0^1(D)$ the closure for the H^1-norm of $C_c^\infty(D)$. Recall that $H_0^1(\mathbb{R}^2) = H^1(\mathbb{R}^2)$. We will use that $H_0^1(D) \subset H^1(\mathbb{R}^2)$, which is a consequence of the inclusion $C_c^\infty(D) \subset C_c^\infty(\mathbb{R}^2)$.

For a function $u \in H_0^1(D)$, we denote

$$\Omega_u = \{x \in D \ : \ u(x) \neq 0\}.$$

Let $|E|$ denote the Lebesgue measure of any measurable subset E of $\mathbb{R}^2$. The value $|\Omega_u|$ does not depend on the choice of the representation of u.

We recall the following Poincaré inequality (see, e.g. [22, Lemme 4.5.3]): there exists a constant C_P such for all $u \in H^1(\mathbb{R}^2)$ satisfying $|\Omega_u| \leq a$, we have

$$\int_{\mathbb{R}^2} u^2 \leq aC_P \int_{\mathbb{R}^2} |\nabla u|^2. \tag{2.1}$$

In particular, if D is a bounded domain, the Poincaré inequality shows that the Hilbertian norm $\|u\|_{H_0^1}^2 = \int_D |\nabla u|^2$ is equivalent to the H^1-norm on $H_0^1(D)$.

We denote (x, z) the cartesian coordinates in the plane $\mathbb{R}^2$. An open set $D \subset \mathbb{R}^2$ is *symmetric* (with respect to the x-axis) if for all $(x, z) \in D$, we have $(x, -z) \in D$. For a function u defined on a symmetric open set D, we will denote $\check{u}$ the function such that $\check{u}(x, z) = u(x, -z)$ for all $(x, z) \in D$. If D is a nonempty symmetric open subset of $\mathbb{R}^2$, we denote $\check{H}(D)$ the following closed subspace of $H_0^1(D)$,

$$\check{H}(D) = \{u \in H_0^1(D),\ \check{u} = u \text{ a.e. in } D\}.$$

From now on and throughout the paper, D denotes a (nonempty) symmetric *bounded* open subset of $\mathbb{R}^2$.

2.2. **The normalized total resistance functional.** For any $u \in \check{H}(\mathbb{R}^2)$ such that $|\Omega_u|$ has finite measure, we consider the functional

$$J(u) = J_0(u) + J_{wave}(u), \tag{2.2}$$

where

$$J_0(u) = \int_{\mathbb{R}^2} |\nabla u(x, z)|^2 dxdz \tag{2.3}$$

and

$$J_{wave}(u) = \frac{4\alpha^4}{\pi C_F(\alpha)} \int_1^\infty |T_u(\lambda)|^2 \frac{\lambda^4}{\sqrt{\lambda^2 - 1}} d\lambda, \tag{2.4}$$

with

$$T_u(\lambda) = \int_{\mathbb{R}^2} u(x, z) e^{-i\lambda\alpha x} e^{-\lambda^2\alpha|z|} dxdz. \tag{2.5}$$

Note that for all $\lambda > 0$, $T_u(\lambda)$ is well-defined by the Cauchy-Schwarz inequality and the Poincaré inequality (2.1). Moreover, the function $\lambda \mapsto T_u(\lambda)$ depends continuously on λ by Lebesgue's dominated convergence theorem.

The functional $J(u)$ represents a normalized version of the resistance of water to the motion of a ship [13]. The Dirichlet energy $J_0(u)$ is obtained by linearization of the area of the hull and it is related to the viscous resistance. The term $J_{wave}(u)$ is a normalization of Michell's wave resistance of the hull [30]. In (2.4)-(2.5), α is the Kelvin wave number (in m^{-1}) and C_F is assumed to be a positive and continuous

function defined on $(0,+\infty)$ ($C_F(\alpha)$ is the viscous drag coefficient and it has no dimension). The integration parameter λ has no dimension: it can be interpreted as $\lambda = 1/\cos\theta$, where θ is an angle at which the wave energy is propagating [25]. The variables x, z and $u(x,z)$ are expressed in meters.

2.3. **Some details on the model.** In Michell's theory [25, 30, 31], it is assumed that the fluid is incompressible, inviscid and that the flow is irrotational. The motion has persisted long enough so that a steady state has been reached. The hull also satisfies the "thin ship" assumptions.

The ship is moving at constant velocity on the surface of an unbounded fluid. A coordinate system fixed with respect to the ship is used. The xy plane is the undisturbed water surface, the positive x axis is in direction of the motion and the z axis is vertically upward. It is assumed that the hull is symmetric with respect to the vertical xz-plane. The immerged half hull is represented by the nonnegative function $y = u(x,z)$ with $x \in \mathbb{R}$ and $z \leq 0$.

Michell's wave resistance of the hull represented by u is given by

$$R_{Michell} = \frac{\rho g}{4\alpha} C_F(\alpha) J_{wave}(u),$$

where ρ (in $\mathrm{kg}\cdot\mathrm{m}^{-3}$) is the constant density of the fluid, g (in $\mathrm{m}\cdot\mathrm{s}^{-2}$) is the standard gravity, and α is related to the speed U of the ship (in $\mathrm{m}\cdot\mathrm{s}^{-1}$) through $\alpha = g/U^2$.

In our model, the viscous resistance is equal to

$$R_{viscous} = \frac{1}{2}\frac{\rho g}{\alpha} C_F(\alpha) \left(|a| + \frac{1}{2} J_0(u) \right)$$

where $|a| = |\Omega_u|$ (in m^2) is (twice) the area of the support of the hull. The total resistance of water to the motion of the ship (expressed in Newtons) reads

$$R_{total} = R_{viscous} + R_{Michell}.$$

We refer the reader to [13] for more details on the model.

2.4. **The nondimensional optimization problem.** Let $V > 0$ (the volume of the hull in m^3) and $a > 0$ (the area of the support of the hull in m^2). We define

$$C_V^{a,+} = \left\{ v \in \check{H}(\mathbb{R}^2) \ : v \geq 0 \text{ a.e. in } \mathbb{R}^2, \ \int_{\mathbb{R}^2} v(x,z)dxdz = V, \text{ and } |\Omega_v| \leq a \right\}.$$

We consider the following optimal design problem:

$$(\mathcal{P}_V^{a,+}) \quad \text{Find } u \in C_V^{a,+} \text{ such that } J(u) \leq J(v), \ \forall v \in C_V^{a,+}.$$

This problem can be simplified by using two scalings. Firstly, we can use that the energy functional is quadratic with respect to u. Thus, we may set the value of V without loss of generality. Roughly speaking, "the" optimal hull u depends linearly on V and the corresponding optimal domain Ω_u is independent of V [13, Remark 3.5].

Secondly, we can use the Froude invariance of the problem. The Froude scaling is well-known for Michell's wave resistance $J_{wave}(u)$ and it turns out that $J_0(u)$ has the same scaling. For our problem, the relevant Froude number Fr is related to the area a through

$$Fr^2 = \frac{1}{\alpha\sqrt{a}} = \frac{U^2}{g\sqrt{a}}. \tag{2.6}$$

In $J(u)$ defined by (2.2), we set

$$x = \sqrt{a}\tilde{x},\ z = \sqrt{a}\tilde{z},\ u(x,z) = \sqrt{a}\tilde{u}(\tilde{x},\tilde{z}),\ \alpha = \tilde{\alpha}/\sqrt{a} \text{ and } C_F(\alpha) = \tilde{C}_F(\tilde{\alpha}). \quad (2.7)$$

This yields $J(u) = a\big(\tilde{J}_0(\tilde{u}) + \tilde{J}_{wave}(\tilde{u})\big)$, where $\tilde{J}_0(\tilde{u})$ and $\tilde{J}_{wave}(\tilde{u})$ have the same expression as $J_0(u)$ (see (2.3)) and $J_{wave}(u)$ (see (2.4)-(2.5)) except that all the variables are replaced by their dimensionless version $\tilde{x}$, $\tilde{z}$, $\tilde{u}(\tilde{x},\tilde{z})$, $\tilde{\alpha}$ and $\tilde{C}_F(\tilde{\alpha})$.

By choosing $V = a^{3/2}$, we see that problem $(\mathcal{P}_V^{a,+})$ is equivalent to problem

$$(\mathcal{P}^+) \quad \text{Find } \tilde{u} \in C^+ \text{ such that } \tilde{J}(\tilde{u}) \le \tilde{J}(\tilde{v}),\ \forall \tilde{v} \in C^+,$$

where $\tilde{J}(\tilde{u}) = \tilde{J}_0(\tilde{u}) + \tilde{J}_{wave}(\tilde{u})$ and

$$C^+ = \left\{ \tilde{v} \in \check{H}(\mathbb{R}^2)\ : \tilde{v} \ge 0 \text{ a.e. in } \mathbb{R}^2,\ \int_{\mathbb{R}^2} \tilde{v}(\tilde{x},\tilde{z})d\tilde{x}d\tilde{z} = 1,\ \text{and } |\Omega_{\tilde{v}}| \le 1 \right\}. \quad (2.8)$$

If $\tilde{u}$ is a solution to problem $(\mathcal{P}^+)$, a solution u_V^a to problem $(\mathcal{P}_V^{a,+})$ is recovered by setting $u_V^a(x,z) = Va^{-1}\tilde{u}(x/\sqrt{a}, z/\sqrt{a})$. In this case, we have

$$J(u_V^a) = \frac{V^2}{a^2}\tilde{J}(\tilde{u}). \quad (2.9)$$

Thus, we may set $a = 1$ and $V = 1$ in problem $(\mathcal{P}_V^{a,+})$, without loss of generality. Alternatively, we may think of the nondimensional problem $(\mathcal{P}^+)$ as problem $(\mathcal{P}_V^{a,+})$ in which $a = 1$ and $V = 1$, so *in the remainder of the paper, we omit the˜ symbol in problem* $(\mathcal{P}^+)$. The optimal domain Ω_u, if it exists, depends only on two parameters without units, namely Fr and C_F.

Using (2.4)-(2.5), it is easy to see that J_{wave} is invariant by translation along the x-axis. Thus, if u is a solution to problem $(\mathcal{P}^+)$, *any translate of* u *along the* x*-axis is also a solution.*

Remark 2.1. Problem $(\mathcal{P}_V^{a,+})$ is related to the following shape optimization problem [13, Remark 3.2]: find an open and symmetric set $\Omega^\star$ such that

$$J(u_{\Omega^\star}) = \inf\left\{ J(u_\Omega),\ \Omega \subset \mathbb{R}^2 \text{ open and symmetric},\ |\Omega| = a \right\}, \quad (2.10)$$

where u_Ω is uniquely defined by

$$J(u_\Omega) = \min\left\{ J(v),\ v \in H_0^1(\Omega),\ \check{v} = v \text{ and } v \ge 0 \text{ a.e. in } \Omega,\ \int_\Omega v = V \right\}. \quad (2.11)$$

2.5. **Introduction of a bounding box.** The analysis and the numerical simulations which follow indicate that problem $(\mathcal{P}^+)$ may have a solution or not, depending on the values of the parameters. In order to simplify the analysis and to have some compactness, we introduce a "bounding box", namely a symmetric bounded open subset D of $\mathbb{R}^2$ such that $|D| > 1$. We replace problem $(\mathcal{P}^+)$ by the simpler problem

$$(\mathcal{P}_D^+) \quad \text{Find } u \in C^+(D) \text{ such that } J(u) \le J(v),\ \forall v \in C^+(D),$$

where

$$C^+(D) = \left\{ v \in \check{H}(D)\ : v \ge 0 \text{ a.e. in } D,\ \int_D v(x,z)dxdz = 1,\ \text{and } |\Omega_v| \le 1 \right\}.$$

By considering a minimizing sequence, it is easy to see that problem $(\mathcal{P}_D^+)$ has at least one solution u [13, Theorem 3.3].

3. Special situations

3.1. **The problem without wave resistance.** We first consider the case where $J(u)$ is replaced by $J_0(u)$ in our optimization problem. We recall a well-known result concerning the following problem:

$$(\mathcal{P}_0) \quad \text{Find } u_0 \in C_0 \text{ such that } J_0(u_0) \leq J_0(v),\ \forall v \in C_0,$$

where

$$C_0 = \left\{ v \in H^1(\mathbb{R}^2) \ : \ \int_{\mathbb{R}^2} v(x,z)dxdz = 1 \text{ and } |\Omega_v| \leq 1 \right\}. \tag{3.1}$$

Theorem 3.1. *Problem $(\mathcal{P}_0)$ has a radial solution u_0, which is unique up to translation in $\mathbb{R}^2$, namely*

$$u_0(x,z) = \begin{cases} 2 - 2\pi r^2 & \text{if } r^2 = x^2 + z^2 < 1/\pi \\ 0 & \text{if } r^2 \geq 1/\pi. \end{cases} \tag{3.2}$$

In particular, $J_0(u_0) = 8\pi$.

Proof. Problem $(\mathcal{P}_0)$ is known as the Saint-Venant problem. We refer the reader to [6] and references therein. A radial solution can be obtain by means of a Schwarz symmetrization. □

Next, we consider problem

$$(\mathcal{P}_D^0) \quad \text{Find } u_D^0 \in C_D^0 \text{ such that } J_0(u_D^0) \leq J_0(v),\ \forall v \in C_D^0,$$

where

$$C_D^0 = \left\{ v \in \check{H}(D) \ : \ \int_D v(x,z)dxdz = 1 \text{ and } |\Omega_v| \leq 1 \right\}.$$

By considering a minimizing sequence, this problem has at least one solution u_D^0 [13, Theorem 3.3]. Moreover, any solution u_D^0 is nonnegative, otherwise the function

$$u^\star = |u_D^0| / \int_D |u_D^0(x,z)|dxdz$$

would belong to C_D^0 and it would satisfy $J_0(u^\star) < J_0(u_D^0)$. The set C_D^0 can therefore be replaced by the set $C^+(D)$ in problem $(\mathcal{P}_D^0)$.

The minimizer u_D^0 can be determined in the following generic situation, which is an immediate consequence of Theorem 3.1 and of the symmetry condition which is imposed in the space $\check{H}(D)$.

Corollary 3.2. *Assume that D contains a disc of area 1 centered at $(x_0, 0)$ (up to a set of zero capacity). Then a solution of $(\mathcal{P}_D^0)$ is given by $u_D^0(x,z) = u_0(x - x_0, z)$ (see (3.2)) and we have $J_0(u_D^0) = 8\pi$. Moreover, u_D^0 is unique up to any translation along the x-axis such that the translate of u_D^0 belongs to $\check{H}(D)$.*

3.2. **Behaviour of the wave resistance functional.** We focus now on the wave resistance functional J_{wave} (2.4). A result of Krein [25] adapted to our context reads:

Theorem 3.3. *The infimum $\inf_{v \in C^+(D)} J_{wave}(v)$ is strictly positive.*

Proof. Assume by contradiction that $\inf_{v\in C^+(D)} J_{wave}(v) = 0$, and let (v_n) denote a minimizing sequence in $C^+(D)$. Then (v_n) is a sequence of nonnegative functions such that $\int_D v_n = V$, so that, up to a subsequence, (v_n) converges in the sense of measures (i.e. weakly-$\star$ in $C^0(\overline{D})'$) to a nonnegative measure $\mu^\star$ on $\overline{D}$ such that $\langle \mu^\star, 1\rangle = V$. In particular, for all $\lambda \in \mathbb{R}$ (see (2.5)),

$$T_{v_n}(\lambda) \to T_{\mu^\star}(\lambda) := \langle \mu^\star, e^{-i\lambda\alpha x} e^{-\lambda^2\alpha|z|}\rangle.$$

By Fatou's lemma,

$$0 \le \frac{4\alpha^4}{\pi C_F(\alpha)} \int_1^\infty |T_{\mu^\star}(\lambda)|^2 \frac{\lambda^4}{\sqrt{\lambda^2-1}} d\lambda \le \liminf_n J_{wave}(v_n) = 0,$$

so that $T_{\mu^\star}(\lambda) = 0$ for all $\lambda \in (1,\infty)$. By analycity (since D is bounded), $T_{\mu^\star}(\lambda) = 0$ for all $\lambda \in \mathbb{R}$. Next, we use that the Fourier transform of a Gaussian density is known:

$$\int_{\mathbb{R}} e^{-\lambda^2\alpha z'} e^{-i\lambda\alpha x} d\lambda = \sqrt{\frac{\pi}{\alpha z'}} e^{-\alpha x^2/(4z')} \quad (z' > 0).$$

We multiply $T_{\mu^\star}(\lambda)$ by $e^{-\lambda^2\alpha}$ and we integrate on $\mathbb{R}$ (this is possible thanks to the new term). By changing the order of integration, we find

$$0 = \langle \mu^\star, \textstyle\int_{\mathbb{R}} e^{-\lambda^2\alpha(|z|+1)} e^{-i\lambda\alpha x} d\lambda\rangle = \langle \mu^\star, \sqrt{\frac{\pi}{\alpha(1+|z|)}} e^{-\alpha x^2/(4(1+|z|))}\rangle.$$

This contradicts $\langle \mu^\star, 1\rangle = V > 0$ and concludes the proof. □

Theorem 3.3 shows that a function $v \in C^+$ with compact support has a strictly positive wave resistance $J_{wave}(v)$. There are schematically two ways of letting $J_{wave}(v)$ tend to 0 while v stays in C^+. One way is to let the support of v get away from the x-axis, as in Theorem 3.5. Physically, this means that the influence of the free surface becomes negligeable as the depth increases. Another possibility is to let the length of the support of v tend to $+\infty$. In this regard, it is instructive to see what happens for a Wigley hull (see, e.g. [31]).

For every $L > 0$ (the length), $T > 0$ (the draft) and $B > 0$ (the beam), we consider the Wigley hull

$$w_{L,T,B}(x,z) = \begin{cases} \dfrac{B}{2}\left(1 - \dfrac{|z|}{T}\right)\left(1 - \dfrac{4x^2}{L^2}\right) & \text{if } |x| \le L/2 \text{ and } |z| \le T, \\ 0 & \text{otherwise} \end{cases}$$

Proposition 3.4. *For each $L > 0$, we set $T_L = 1/(2L)$ and $B_L = 6$. Then we have*

$$\int_{\mathbb{R}^2} w_{L,T_L,6}(x,z)dxdz = 1,\ \Omega_{w_{L,T_L,6}} = 1 \quad \textit{and} \quad J_{wave}(w_{L,T_L,6}) \to 0 \ \textit{as}\ L \to +\infty.$$

Proof. The Wigley hull $w_{L,T,B}$ has a rectangular support with area $2LT$ and its volume is

$$\int_{\mathbb{R}^2} w_{L,T,B}(x,z)dxdz = BLT/3.$$

A computation yields

$$T_{w_{L,T,B}}(\lambda) = B\, I_1(\lambda)\, I_2(\lambda)$$

with

$$0 \le I_2(\lambda) = \int_0^T e^{-\lambda^2\alpha z}(1 - z/T)dz \le \int_0^T e^{-\lambda^2\alpha z} dz = \frac{1 - e^{-\lambda^2\alpha T}}{\alpha\lambda^2}$$

and

$$I_1(\lambda) = \int_{-L/2}^{L/2} \left(1 - \frac{4x^2}{L^2}\right) e^{-i\lambda\alpha x} dx = -\frac{8}{\lambda^2\alpha^2 L}\left[\cos\left(\frac{\lambda\alpha L}{2}\right) - \frac{2}{\lambda\alpha L}\sin\left(\frac{\lambda\alpha L}{2}\right)\right].$$

For $\lambda \geq 1$ we have

$$|I_1(\lambda)| \leq \frac{8}{\lambda^2\alpha^2 L}\left(1 + \frac{2}{\alpha L}\right) \text{ and } |I_2(\lambda)| \leq \frac{1}{\alpha\lambda^2},$$

and from (2.4), we deduce that

$$J_{wave}(w_{L,T,B}) \leq \frac{256B^2}{\pi C_F(\alpha)\alpha^2 L^2}\left(1 + \frac{2}{\alpha L}\right)^2 \int_1^\infty \frac{d\lambda}{\lambda^4\sqrt{\lambda^2 - 1}}.$$

The claim follows by choosing $T = 1/2L$, $B = 6$ and by letting L tend to $+\infty$. □

Figure 1 shows the behaviour of $J_{wave}(w_{L,T_L,6})$ as a function of L for area Froude numbers $Fr = 0.3$, 0.4 and 0.5 (cf. (2.6)). In this numerical computation, the coefficient C_F was set equal to 0.01. It confirms that it can be very interesting to increase the length of the domain.

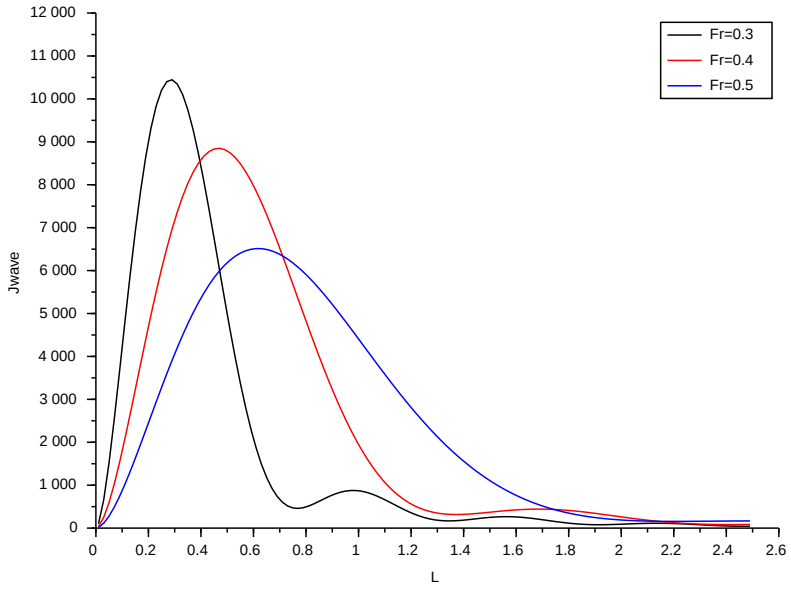

FIGURE 1. $J_{wave}(w_{L,T_L,6})$ vs. L

3.3. **A nonexistence result.** If D is unbounded, problem $(\mathcal{P}_D^+)$ may have no solution, as shown by the following result. We denote $\mathbb{R}^\star = \mathbb{R} \setminus \{0\}$ and

$$C^+(\mathbb{R}\times\mathbb{R}^\star) = \left\{v \in \check{H}(\mathbb{R}\times\mathbb{R}^\star) \ : \ v \geq 0 \text{ a.e., } \int_{\mathbb{R}\times\mathbb{R}^\star} v = 1 \text{ and } |\Omega_v| \leq 1\right\}.$$

Theorem 3.5. *We have* $\inf_{v\in C^+(\mathbb{R}\times\mathbb{R}^\star)} J(v) = 16\pi$ *and this infimum is not attained. A minimizing sequence is obtained by setting*

$$v_n(x,z) = \begin{cases} 2 - 4\pi((x^2 + (z-z_n)^2) & \text{if } x^2 + (z-z_n)^2 < 1/(2\pi) \\ 2 - 4\pi((x^2 + (z+z_n)^2) & \text{if } x^2 + (z+z_n)^2 < 1/(2\pi) \\ 0 & \text{otherwise} \end{cases} \tag{3.3}$$

and by letting z_n *tend to* $+\infty$.

Proof. By symmetry, a function $u^\star$ is a minimizer of J_0 in the set $C^+(\mathbb{R}\times\mathbb{R}^\star)$ if and only if its restriction $u^\star_{|\mathbb{R}\times(0,+\infty)}$ to the open set $\mathbb{R}\times(0,+\infty)$ is a minimizer of J_0 in the set

$$\{v \in H^1_0(\mathbb{R}\times(0,+\infty)) \ : \ v \geq 0 \text{ a.e. }, \ |\Omega_v| \leq 1/2, \ \int_{\mathbb{R}\times(0,+\infty)} v = 1/2\}.$$

By Theorem 3.1 and scaling arguments, for any $z_n \geq \sqrt{1/(2\pi)}$ the function v_n defined by (3.3) is such a minimizer and $J_0(v_n) = 16\pi$. By construction,

$$J(v) = J_0(v) + J_{wave}(v) \geq J_0(v), \tag{3.4}$$

for all $v \in \check{H}(\mathbb{R}\times\mathbb{R}^\star)$, so that

$$\inf_{v\in C^+(\mathbb{R}\times\mathbb{R}^\star)} J(v) \geq \inf_{v\in C^+(\mathbb{R}\times\mathbb{R}^\star)} J_0(v) = 16\pi.$$

For $z_n > \sqrt{1/(2\pi)}$, we have

$$|T_{v_n}(\lambda)| \leq \int_{\mathbb{R}\times\mathbb{R}^\star} |v_n(x,z)| e^{-\lambda^2\alpha|z|} dxdz \leq V e^{-\lambda^2\alpha(z_n - \sqrt{1/(2\pi)})},$$

so that $J_{wave}(v_n) \to 0$ as $z_n \to +\infty$. This shows that

$$\inf_{v\in C^+(\mathbb{R}\times\mathbb{R}^\star)} J(v) = J_0(v_n) = 16\pi.$$

Now we assume by contradiction that $J(u^\star) = 16\pi$ for some $u^\star \in C^+(\mathbb{R}\times\mathbb{R}^\star)$. Then by (3.4) we have $J_0(u^\star) = 16\pi$ and $J_{wave}(u^\star) = 0$. In particular, $u^\star$ is a minimizer of J_0 in $C^+(\mathbb{R}\times\mathbb{R}^\star)$. The uniqueness result in Theorem 3.1 and the symmetry argument above imply that $u^\star$ is either a function v_n or the translate of a function v_n in the x direction, for some $z_n \geq \sqrt{1/(2\pi)}$. In particular, $u^\star$ has a compact support. For such a function, Theorem 3.3 shows that $J_{wave}(u^\star) > 0$, yielding a contradiction. The proof is complete. □

Theorem 3.5 and Theorem 3.1 imply that

$$\inf_{v\in C^+} J(v) \in [8\pi, 16\pi]. \tag{3.5}$$

4. Continuity with respect to the speed

4.1. **Michell's wave resistance kernel.** By formally switching the integrals in the expression (2.4)-(2.5), we see that Michell's normalized wave resistance can be written

$$J_{wave}(u) = \int_{\mathbb{R}^2\times\mathbb{R}^2} k_\alpha(x,z,x',z') u(x,z) u(x',z') dxdzdx'dz' \tag{4.1}$$

where

$$k_\alpha(x,z,x',z') = \frac{4\alpha^4}{\pi C_F(\alpha)} k(\alpha(x-x'), \alpha(|z| + |z'|)) \tag{4.2}$$

and

$$k(X,Z)=\int_1^\infty e^{-\lambda^2 Z}\cos(\lambda X)\frac{\lambda^4}{\sqrt{\lambda^2-1}}d\lambda. \tag{4.3}$$

This formal calculation was rigorously proved in [13, Appendix A]. It was shown that Michell's kernel belongs to $L^{5/4-\varepsilon}(D\times D)$ and that this estimate is optimal if D contains an open disc centered on the x-axis.

The results from [13, Appendix A] are summarized in the proposition below. We first note that k is defined and continuous on $\mathbb{R}\times(0,+\infty)$, thanks to the exponential term, so that k_α is continuous on $(\mathbb{R}\times\mathbb{R}^\star)^2$.

Proposition 4.1. *Michell's normalized wave resistance kernel k_α (4.2) belongs to $L^q(D\times D)$ for all $1\le q<5/4$. For each $q'>5$ and for each $u\in L^{q'}(D)$, the formulations for $J_{wave}(u)$ given by (2.4)-(2.5) and (4.1)-(4.2)-(4.3) are equal.*

Let $q\in(1,5/4)$ and let $q'=q/(q-1)\in(5,+\infty)$ be the conjugate exponent of q. By Hölder's inequality, we have

$$\int_D\int_D |k_\alpha(x,z,x',z')u(x,z)v(x',z')|dxdzdx'dz'\le \|k_\alpha\|_{L^q(D\times D)}\|u\|_{L^{q'}(D)}\|v\|_{L^{q'}(D)}, \tag{4.4}$$

for all $u,v\in L^{q'}(D)$. Since $H^1_0(D)$ is continuously imbedded in $L^{q'}(D)$ for all $q'\in[1+\infty)$ [16], this shows that for all $u\in\check{H}(D)$, $J_{wave}(u)<+\infty$.

4.2. **Continuity of the optimal hull with respect to the speed.** In this section, we show that "the" solution u of problem $(\mathcal{P}_D^+)$ depends continuously (up to uniqueness) on the Froude number Fr through $\alpha=1/Fr^2$ (i.e. on the speed U of the ship, since $Fr^2=U^2/g\sqrt{a}$, cf. Section 2.4). For this purpose, a good approach is the Γ-convergence of the functionals in H^1 [5, 22].

In order to stress the dependence on α, we denote J^α_{wave} Michell's normalized wave resistance (2.4); T^α_u is the corresponding operator (2.5), the normalized total resistance is $J^\alpha=J_0+J^\alpha_{wave}$, and problem $(\mathcal{P}_D^+)$ is denoted $(\mathcal{P}^+_{D,\alpha})$. We recall that $C_F:(0,+\infty)\to(0,+\infty)$ is a positive function which depends continuously on α.

The following lemma provides a Γ-convergence result for the weak H^1-topology (in any bounded subset of $\check{H}(D)$ which is weakly closed).

Lemma 4.2. *Let α,α_n be positive real numbers such that $\alpha_n\to\alpha$. Then,*

(i) *For every sequence (u_n) in $\check{H}(D)$ which converges weakly in $H^1_0(D)$ to some u, $J^\alpha_{wave}(u)\le\liminf_n J^{\alpha_n}_{wave}(u_n)$, and*
(ii) *For every $u\in\check{H}(D)$, $J^{\alpha_n}_{wave}(u)\to J^\alpha_{wave}(u)$.*

Proof. Let (u_n) be a sequence in $\check{H}(D)$ which converges weakly in $H^1_0(D)$ to some u. Then (u_n) converges weakly in $L^2(D)$ to u and the functions $(x,z)\mapsto e^{-i\lambda\alpha_n x}e^{-\lambda^2\alpha_n|z|}$ converge uniformly in D to the function $(x,z)\mapsto e^{-i\lambda\alpha x}e^{-\lambda^2\alpha|z|}$, so that $T^{\alpha_n}_{u_n}(\lambda)\to T^\alpha_u(\lambda)$, for every $\lambda\in(1,+\infty)$. By Fatou's lemma,

$$\int_1^\infty |T^\alpha_u(\lambda)|^2\frac{\lambda^4}{\sqrt{\lambda^2-1}}d\lambda\le\liminf_n\int_1^\infty \left|T^{\alpha_n}_{u_n}(\lambda)\right|^2\frac{\lambda^4}{\sqrt{\lambda^2-1}}d\lambda.$$

Since C_F is a positive and continuous function, this proves point (i).

Let now $u \in \check{H}(D)$. In order to prove point (ii), we use that J^α_{wave} can be expressed in terms of the kernel k_α, cf. Proposition 4.1. Performing the change of variable $(\tilde{x}, \tilde{z}, \tilde{x}', \tilde{z}') = \alpha(x, z, x', z')$ in (4.1), we find that

$$J^\alpha_{wave}(u) = \frac{4}{\pi C_F(\alpha)} \int_{\alpha D \times \alpha D} k(x - x', |z| + |z'|) u(\frac{x}{\alpha}, \frac{z}{\alpha}) u(\frac{x'}{\alpha}, \frac{z'}{\alpha}) dx dz dx' dz'. \quad (4.5)$$

Since $\alpha_n \to \alpha > 0$, the domains $\alpha_n D$, αD are all contained in an open disc B_l of radius $l > 0$ large enough and centered at $(0, 0)$. Thus, since $u \in H^1_0(D)$,

$$J^{\alpha_n}_{wave}(u) = \frac{4}{\pi C_F(\alpha_n)} \int_{B_l} k(x - x', |z| + |z'|) u(\frac{x}{\alpha_n}, \frac{z}{\alpha_n}) u(\frac{x'}{\alpha_n}, \frac{z'}{\alpha_n}) dx dz dx' dz'. \quad (4.6)$$

By Proposition 4.1, k_1 belongs to $L^q(B_l \times B_l)$ for some $1 < q < 5/4$. Moreover, the sequence of functions $u_n(x, z) = u(\frac{x}{\alpha_n}, \frac{z}{\alpha_n})$ converges strongly in $L^{q'}(B_l)$ to $u(\frac{x}{\alpha}, \frac{z}{\alpha})$. By (4.4) and the continuity of C_F, the right-hand side of (4.6) converges to the right-hand side of (4.5), i.e. $J^{\alpha_n}_{wave}(u) \to J^\alpha_{wave}(u)$, as claimed. □

From this, we deduce:

Theorem 4.3. *Let α, α_n be positive real numbers such that $\alpha_n \to \alpha$ and for every n, let u_n denote a solution of problem $(\mathcal{P}^+_{D,\alpha_n})$. Then, up to a subsequence, (u_n) converges strongly in $H^1_0(D)$ to a solution u of problem $(\mathcal{P}^+_{D,\alpha})$.*

Proof. Let u_α denote a solution of problem $(\mathcal{P}^+_{D,\alpha})$. Then

$$J^{\alpha_n}(u_n) = J_0(u_n) + J^{\alpha_n}_{wave}(u_n) \leq J^{\alpha_n}(u_\alpha), \quad (4.7)$$

and $J^{\alpha_n}(u_\alpha)$ is bounded by a constant independent of n, by point (ii) of Lemma 4.2. This shows that (u_n) is bounded in $H^1_0(D)$ so, up to a subsequence, (u_n) converges weakly in $H^1_0(D)$ to some u, which belongs to $\check{H}(D)$. By Rellich's theorem, (u_n) converges to u strongly in $L^2(D)$ and (up to a subsequence) a.e. in D. Thus, $u \geq 0$ a.e. in D and $\int_D u = V$. We have $\chi_{\Omega_u} \leq \liminf_n \chi_{\Omega_{u_n}}$ a.e. in D, so by Fatou's lemma,

$$|\Omega_u| = \int_D \chi_{\Omega_u} \leq \liminf_n \int_D \chi_{\Omega_{u_n}} = \liminf_n |\Omega_{u_n}| \leq 1.$$

This shows that u belongs to $C^+(D)$. By semi-continuity of J_0, and by point (i) of Lemma 4.2,

$$J^\alpha(u) = J_0(u) + J^\alpha_{wave}(u) \leq \liminf_n J_0(u_n) + \liminf_n J^{\alpha_n}_{wave}(u_n) \leq \liminf_n J^{\alpha_n}(u_n).$$

Using (4.7) and point (ii) of Lemma 4.2, we also have

$$\liminf_n J^{\alpha_n}(u_n) \leq J^\alpha(u_\alpha).$$

Thus, $J^\alpha(u) \leq J^\alpha(u_\alpha)$, and so u is a solution of problem $(\mathcal{P}^+_{D,\alpha})$. By (4.7) and Lemma 4.2 again, we have

$$\limsup_n J_0(u_n) \leq \lim_n J^{\alpha_n}(u_\alpha) - \liminf_n J^{\alpha_n}_{wave}(u_n) \leq J^\alpha(u_\alpha) - J^\alpha_{wave}(u) = J_0(u),$$

and so $J_0(u_n) \to J_0(u)$. Thus, (u_n) converges to u strongly in $H^1_0(D)$ and the proof is complete. □

4.3. **Behaviour for large speeds.** The following Γ-convergence result implies that when $\alpha \to 0$, the contribution of the wave resistance disappears if C_F is constant or if $1/C_F(\alpha)$ has a logarithmic growth, as in the ITTC 1957 model-ship correlation line [3, Equation (2.18)].

Lemma 4.4. *Assume that $\alpha/C_F(\alpha) \to 0$ as $\alpha \to 0^+$. Then for every $u \in \check{H}(D)$, $J^\alpha_{wave}(u) \to 0$ as $\alpha \to 0^+$.*

Proof. We let $l > 0$ be large enough so that $D \subset (-l,l)^2$. The space $\check{H}(D)$ can be seen as a subspace of $H^1_0((-l,l)^2)$. Let $u \in \check{H}(D)$. Then u, being an element of $H^1_0((-l,l)^2)$, has a trace on $(-l,l)\times\{0\}$ which belongs to $L^2(-l,l)$ [7]. Using the symmetry of u and integrating by parts with respect to z in (2.5), we find

$$T^\alpha_u(\lambda) = \frac{1}{\lambda^2\alpha}\left[A^\alpha_u(\lambda) + B^\alpha_u(\lambda)\right], \tag{4.8}$$

with

$$A^\alpha_u(\lambda) = 2\int_{-l}^{l} u(x,0)e^{-i\lambda\alpha x}dx \quad \text{and} \quad B^\alpha_u(\lambda) = 2\int_{D^+} u_z(x,z)e^{-i\lambda\alpha x}e^{-\lambda^2\alpha z}dxdz. \tag{4.9}$$

Here, we denote $D^+ = D \cap \{(x,z)\in\mathbb{R}^2 \ : z>0\}$. From (2.4) and (4.8), we deduce

$$\begin{aligned} J^\alpha_{wave}(u) &= \frac{4\alpha^4}{\pi C_F(\alpha)}\int_1^2 |T^\alpha_u(\lambda)|^2 \frac{\lambda^4}{\sqrt{\lambda^2-1}}d\lambda \\ &\quad + \frac{4\alpha^2}{\pi C_F(\alpha)}\int_2^\infty |A^\alpha_u(\lambda)+B^\alpha_u(\lambda)|^2 \frac{1}{\sqrt{\lambda^2-1}}d\lambda. \end{aligned} \tag{4.10}$$

We have $|T^\alpha_u(\lambda)| \le \|u\|_{L^1(D)} \le |D|^{1/2}\|u\|_{L^2(D)}$ for all $\lambda \in (1,2)$, so that by the assumption on C_F, the first term in the right-hand side of (4.10) tends to 0 as $\alpha \to 0^+$. For the second term, we use that

$$\begin{aligned} &\frac{4\alpha^2}{\pi C_F(\alpha)}\int_2^\infty |A^\alpha_u(\lambda)+B^\alpha_u(\lambda)|^2 \frac{1}{\sqrt{\lambda^2-1}}d\lambda \\ &\le \frac{8\alpha}{\pi C_F(\alpha)}\int_2^\infty \left|\sqrt{\alpha}A^\alpha_u(\lambda)\right|^2 \frac{1}{\sqrt{\lambda^2-1}}d\lambda \\ &\quad + \frac{8\alpha}{\pi C_F(\alpha)}\int_2^\infty \left|\sqrt{\alpha}B^\alpha_u(\lambda)\right|^2 \frac{1}{\sqrt{\lambda^2-1}}d\lambda. \end{aligned} \tag{4.11}$$

We will prove that $\sqrt{\alpha}A^\alpha_u$ and $\sqrt{\alpha}B^\alpha_u$ are bounded in

$$L^2((2,+\infty), d\lambda/\sqrt{\lambda^2-1}),$$

i.e. the space of complex-valued square integrable functions with respect to the measure $d\lambda/\sqrt{\lambda^2-1}$ on $(2,+\infty)$. The assumption on C_F implies then that every term in (4.11) tends to 0 as α tends to 0^+, and the proof will be complete.

Letting $x' = \alpha x$ in the definition of A^α_u, we find

$$\sqrt{\alpha}A^\alpha_u(\lambda) = \frac{2}{\sqrt{\alpha}}\int_{-\alpha l}^{\alpha l} u(x'/\alpha,0)e^{-i\lambda x'}dx' = \mathcal{F}\left(\frac{2}{\sqrt{\alpha}}v_u(\frac{\cdot}{\alpha})\right), \tag{4.12}$$

where $v_u : \mathbb{R}\to\mathbb{R}$ is the trace of u on $(-l,l)$ and 0 on $\mathbb{R}\setminus(-l,l)$, and $\mathcal{F} : L^2(\mathbb{R};\mathbb{C}) \to L^2(\mathbb{R};\mathbb{C})$ is the Fourier transform (a linear bounded operator). But

$\|\frac{2}{\sqrt{\alpha}}v_u(\frac{\cdot}{\alpha})\|_{L^2(\mathbb{R})} = \|2v_u(\cdot)\|_{L^2(\mathbb{R})}$, so the family $\frac{2}{\sqrt{\alpha}}v_u(\frac{\cdot}{\alpha})$ is bounded in $L^2(\mathbb{R})$, and $\sqrt{\alpha}A_u^\alpha$ as well. Finally, since $\sqrt{\lambda^2-1} \geq 1$ for all $\lambda \geq 2$, we have

$$\|\sqrt{\alpha}A_u^\alpha\|_{L^2((2,+\infty),d\lambda/\sqrt{\lambda^2-1})} \leq \|\sqrt{\alpha}A_u^\alpha\|_{L^2((2,+\infty),d\lambda)} \leq \|\sqrt{\alpha}A_u^\alpha\|_{L^2(\mathbb{R})},$$

and so $\sqrt{\alpha}A_u^\alpha$ is bounded in $L^2((2,+\infty), d\lambda/\sqrt{\lambda^2-1})$, as claimed.

By the Cauchy-Schwarz inequality, we have

$$\begin{aligned} |\sqrt{\alpha}B_u^\alpha(\lambda)| &\leq 2\sqrt{\alpha}\|u_z\|_{L^2(D^+)}\|e^{-\lambda^2\alpha z}\|_{L^2(D^+)}, \\ &\leq 2\|u_z\|_{L^2(D)}\frac{\sqrt{l}}{\lambda}. \end{aligned} \tag{4.13}$$

Thus, $\sqrt{\alpha}B_u^\alpha$ is bounded in $L^2((2,+\infty), d\lambda/\sqrt{\lambda^2-1})$, as claimed. The lemma is proved. □

Arguing as in the proof of Theorem 4.3, from Lemma 4.4 we deduce:

Theorem 4.5. *Assume that $\alpha/C_F(\alpha) \to 0$ as $\alpha \to 0^+$, let (α_n) be a sequence of positive real numbers such that $\alpha_n \to 0$, and for every n, let u_n denote a solution of problem $(\mathcal{P}^+_{D,\alpha_n})$. Then, up to a subsequence, (u_n) converges strongly in $H^1_0(D)$ to a solution u_D^0 of problem $(\mathcal{P}^0_D)$.*

Remark 4.6. The minimizers u_D^0 have been determined when D contains a disc of area 1 centered on the x-axis (Corollary 3.2).

Remark 4.7. Assume that C_F is constant. Then it is easy to see that for all $u \in C_c^\infty(D) \cap \check{H}(D)$, $J^\alpha_{wave}(u) \to 0$ as $\alpha \to +\infty$. However, we have not been able to prove that a sequence (u_n) of solutions to problem $(\mathcal{P}^+_{D,\alpha_n})$ converges to a solution u_D^0 when $\alpha_n \to +\infty$.

5. Numerical methods

In order to study numerically how the optimal shape depends on the Froude number, we have computed solutions to problem $(\mathcal{P}^+)$. We describe here the shape optimization gradient algorithm that was used (see also [13, Section 8] and [1, Section 6.5]).

We stress that we used the dimensional form of the problem for the algorithm. Our computation first provides a numerical solution to a problem $(\mathcal{P}^{a,+}_V)$. Then, we apply the scalings described in Section 2.4 and we recover a solution to the nondimensional problem $(\mathcal{P}^+)$. In particular, *the Froude invariance ensures that the area of the computed optimal domain is equal to* 1.

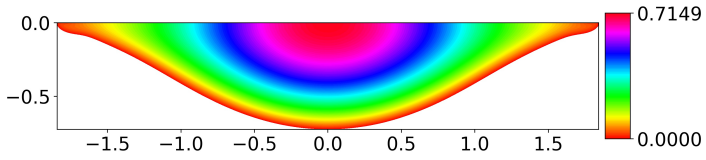

Figure 2. Optimal domain for $Fr = 0.46$

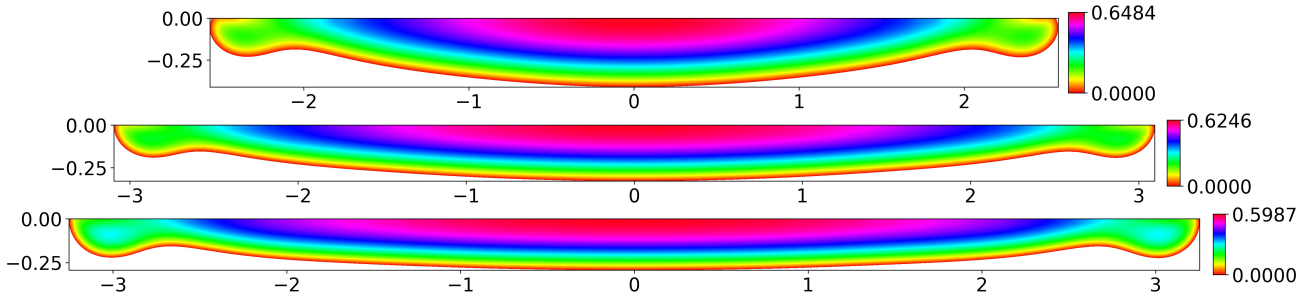

FIGURE 3. Optimal domain for $Fr = 0.67$ (top), 0.81 (middle) and 0.98 (bottom)

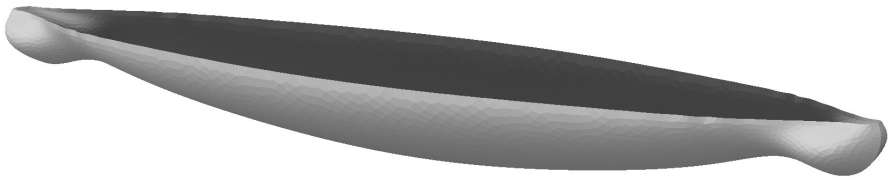

FIGURE 4. Optimal hull for $Fr = 0.67$

5.1. **Shape derivative.** For the numerical resolution of problem $(\mathcal{P}_V^{a,+})$, we use the formulation (2.10), where u_Ω is the unique solution of

$$J(u_\Omega) = \min\left\{ J(v),\ v \in H_0^1(\Omega),\ \check{v} = v \text{ a.e. in } \Omega \text{ and } \int_\Omega v = V \right\}. \tag{5.1}$$

Note that if the solution u_Ω of (5.1) is nonnegative, then u_Ω also solves (2.11). In all the numerical simulations presented below, *the nonnegativity of u_Ω was checked numerically.*

Using Michell's kernel k_α (4.2), a standard argument [13] shows that the solution $u_\Omega \in \check{H}(\Omega)$ to (5.1) is the unique solution to the linear boundary value problem

$$\begin{cases} -\Delta u_\Omega(x,z) + \int_\Omega k_\alpha(x,z,x',z') u_\Omega(x',z') dx'dz' = C, & (x,z) \in \Omega, \\ \int_\Omega u_\Omega(x,z) dxdz = V. \end{cases} \tag{5.2}$$

The constant $C \in \mathbb{R}$ is the Lagrange multiplier associated to the volume constraint.

As a shortcut, we denote $\mathcal{J}(\Omega) = J(u_\Omega)$ the shape functional. Assume that Ω is a symmetric bounded subset of $\mathbb{R}^2$ with smooth boundary $\partial\Omega$. The shape derivative $\mathcal{J}'(\Omega)$ of $\mathcal{J}$ at Ω is the differential in $W^{1,\infty}(\mathbb{R}^2, \mathbb{R}^2)$ of the functional

$$\theta \mapsto \mathcal{J}\big((Id + \theta)(\Omega)\big).$$

A standard computation [1, 22] shows that

$$\mathcal{J}'(\Omega)(\theta) = -\int_{\partial\Omega} \theta \cdot n \left(\frac{\partial u_\Omega}{\partial n}\right)^2 d\sigma,$$

where n is the exterior normal to $\partial\Omega$.

We only allow variations θ for which the domain $(Id + \theta)(\Omega)$ is symmetric, i.e. such that $\theta = (\theta_1, \theta_2)$ satisfies

$$\theta_1(x, -z) = \theta_1(x, z) \text{ and } \theta_2(x, -z) = -\theta_2(x, z) \text{ for a.e. } (x, z) \in \mathbb{R}^2. \tag{5.3}$$

We denote $\check{W}$ the subspace of variations $\theta \in W^{1,\infty}(\mathbb{R}^2, \mathbb{R}^2)$ which fulfill the symmetry conditions (5.3).

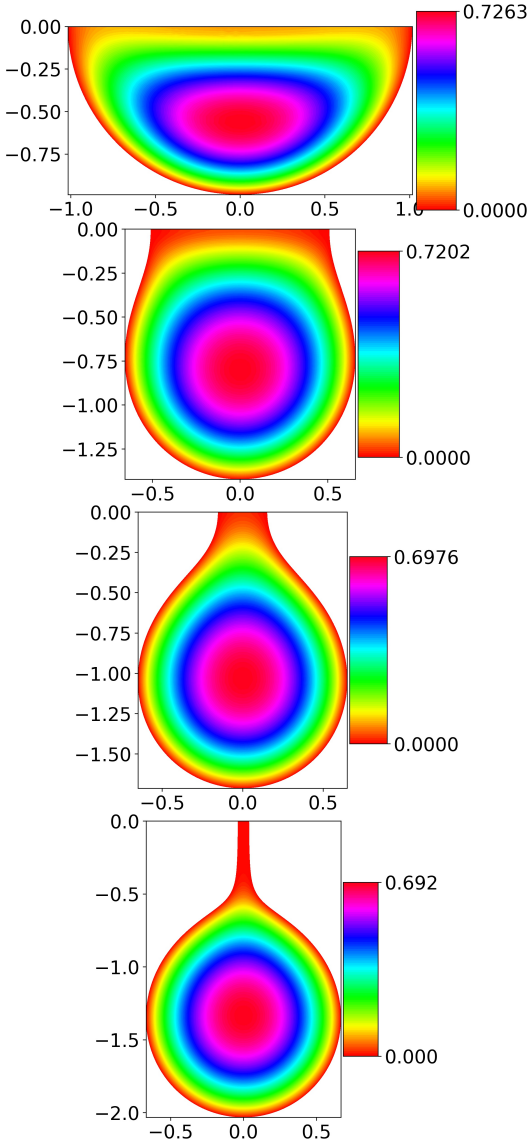

FIGURE 5. A minimizing sequence for $Fr = 1.75$ (sinking case)

5.2. **Shape optimization gradient algorithm.** The algorithm starts with an initial domain Ω_0. For $k = 0, 1, 2, \ldots$ until convergence, the domain Ω_{k+1} is computed as follows:

(1) Compute the solution u_{Ω_k} to (5.2) on Ω_k.

FIGURE 6. Optimal hull built on a half disc for $Fr = 1.75$ (3D view of Figure 5-top)

(2) Compute the descent direction $\theta_k \in \check{W}$ which solves

$$\begin{cases} 0.1\theta_k - \Delta\theta_k = 0 & \text{in } \Omega_k \\ \frac{\partial\theta_k}{\partial n} = \left(\left(\frac{\partial u_{\Omega_k}}{\partial n_k} \right)^2 - \lambda_k \right) n_k & \text{on } \partial\Omega_k. \end{cases} \tag{5.4}$$

where n_k is the outward normal to Ω_k and

$$\lambda_k = \frac{1}{2}\lambda_{k-1} + \frac{1}{2}\frac{1}{\int_{\partial\Omega_k} d\sigma} \int_{\partial\Omega_k} \left(\frac{\partial u_{\Omega_k}}{\partial n_k} \right)^2 d\sigma + 2\frac{|\Omega_k| - |\Omega_0|}{|\Omega_0|}.$$

(3) Set $\Omega_{k+1} = (Id + \mu_k\theta_k)(\Omega_k)$, where $\mu_k = 0.05$ is the constant step size.

Due to the Neumann boundary condition in (5.4), θ_k is a regularization of the shape gradient. Moreover, θ_k is a descent direction of $\mathcal{J}$ associated to the area constraint [1, p. 159]. The area constraint $|\Omega_k| = a$ is dealt with thanks to the Lagrange multiplier λ_k. It is only satisfied at convergence.

No bounding box D is used. The algorithm is stopped when two successive values of the resistance $J(u_{\Omega_k})$ are close enough and when the shape gradient is small enough. The optimal domain usually depends on the choice of the initial domain. In some cases, the algorithm did not converge and it was stopped after a maximal number of steps.

In order to take advantage of the symmetry of the domain about the x-axis, the gradient algorithm is only performed on the lower half of the domain Ω_k. This corresponds to the initial optimization problem of finding an optimal ship hull [13]. It divides by two the number of unknowns. For the space discretization, we used at every step k the same mesh for the computation of u_{Ω_k} and θ_k, because the computation of the full matrix associated to Michell's kernel is costly. A remeshing is performed for Ω_{k+1}.

We validated our algorithm by solving problem $(\mathcal{P}_0)$ numerically. The optimal domain that we obtained was a half disc, in agreement with Theorem 3.1. The relative error between the numerical value of the infimum of J_0 and its theoretical value was less than 0.001. The computation of the wave-resistance J_{wave} was tested on Wigley hulls and compared with values in the literature [14].

6. NUMERICAL RESULTS

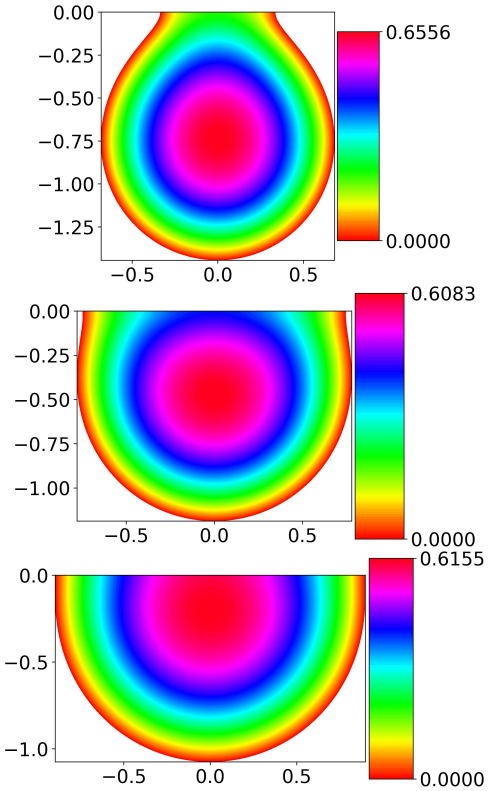

FIGURE 7. Optimal domain for $Fr = 2.45$ (top), 3.15 (middle) and 4.90 (bottom)

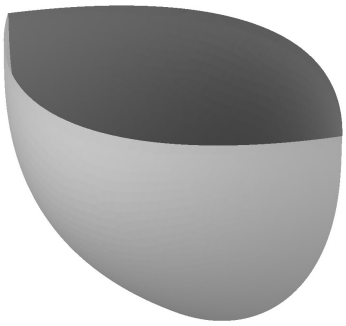

FIGURE 8. Optimal hull for $Fr = 4.90$

6.1. **Optimal domains.** We have computed numerically the optimal solution u to problem $(\mathcal{P}^+)$ for different values of the area Froude number Fr (2.6). The viscous drag coefficient C_F was set to 0.01, except in Figure 10 and Section 6.3.

In Figures 2-7, the optimal domain is represented in variables $\sqrt{\pi}\tilde{x}, \sqrt{\pi}\tilde{z}$ where $\tilde{x}, \tilde{z}$ are defined in (2.7). In these figures, the level sets of the optimal hull are also represented for a same normalized volume V. If we use units, these figures represent the solution to problem $(\mathcal{P}_V^{a,+})$ for $a = \pi$ (m^2) and $V = \pi/3$ (m^3). The choice $a = \pi$ allows an easy comparison with a disc of radius one, as computed in Figure 5 (top).

6.1.1. *Froude numbers smaller than* 1. We first computed the optimal solution for $Fr = 0.67$ in Figure 3 (top) and Figure 4. We see that the optimal hull in this case has a bulbous bow. It is also even with respect to the z-axis. This can easily be related to the symmetry of the functional J if the domain is assumed to be symmetric [14], but proving the symmetry of the optimal domain seems out of reach.

The optimal domains for Froude numbers between 0.5 and 1 have a similar shape, as can be seen in Figure 3. We recover here that these values of the Froude number correspond to the situation where the contribution of the wave-resistance is most important [2, 34] and where a bulbous bow is most interesting.

For Froude numbers smaller than 0.5, the contribution of the wave resistance becomes small (Figure 2), as partially predicted, cf. Remark 4.7.

In Table 1, we have computed the length L of the optimal domain with area 1 for several Froude numbers in $[0.34, 0.98]$. We have also computed the length Froude number Fr_L of the optimal domain defined by

$$Fr_L^2 = \frac{U^2}{gL} = \frac{\sqrt{a}}{L} Fr^2.$$

We see that the length of the optimal domain increases as the Froude number increases. This agrees with the importance of the length in ship hull design [25].

In a simplified model where only the ship's bow and stern are sources of wave formation, the optimal length Froude number has a typical value corresponding to a favorable interference of the transverse waves generated by the ship [25, pp. 325–326] (cf. also [12]). The model here is more complex regarding the geometry, so that the length Froude number Fr_L is not exactly constant. The situation is even more complicated in reality, but statistical observations can be gathered concerning the main characteristics of ship hulls. In [4], a simple model involving Michell's wave resistance explains these observations.

Fr	0.34	0.46	0.58	0.67	0.74	0.81	0.89	0.98
$\sqrt{\pi}L$	2.82	3.69	4.73	5.12	5.81	6.19	6.43	6.50
Fr_L	0.27	0.32	0.35	0.39	0.41	0.43	0.47	0.51

TABLE 1. Comparison of the area Froude number Fr, the length L of the optimal domain and the length Froude number Fr_L ($a = 1$)

6.1.2. *Large Froude numbers.* For large Froude numbers, the contibution of the wave resistance vanishes and the optimal domain ressembles a half disc, in agreement with Theorem 4.5. This can be seen for $Fr = 4.90$ in Figure 7 (bottom) and Figure 8.

As the Froude number decreases from 4.90, the contribution of the wave resistance becomes more important. The center of gravity of the optimal domain decreases along with the Froude number, as shown in Figure 7 for $Fr = 4.90$, $Fr = 3.15$ and $Fr = 2.45$. Here, the wave resistance decreases by increasing the typical depth of the optimal domain. This is very different from the bulbous bow which is related to the length, as seen previously.

6.1.3. *Intermediate Froude numbers.* For $Fr \in [1.1, 2.1]$, we did not find any stable minimizer to the problem. Instead, starting with a half disc, the algorithm produced a minimization sequence similar to the one built in Theorem 3.5. This is shown

in Figure 5 for $Fr = 1.75$. For these values of the Froude number, problem $(\mathcal{P}^+)$ does not seem to have a solution. The wave resistance functional goes to zero as the domain "sinks".

We think that this "sinking" phenomenon can be related to the midship bulbs obtained by some authors such as Hsiung [23, 24] and Gotman [18]. They used a similar model based on Michell's wave resistance in the case of a fixed domain. The midship bulb is clearly observed in Figure 6 where we see the optimal hull for $Fr = 1.75$ when the domain is a half disc (the half disc is not optimal in this case).

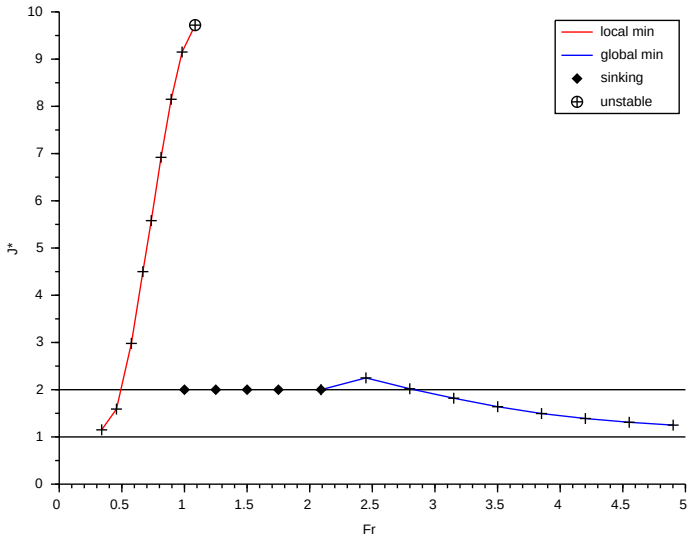

FIGURE 9. $J^\star$ vs Fr ($C_F = 0.01$)

6.2. **Value of the infimum.** The three different possibilities for the optimal domain are obvious in Figure 9. Let us consider the infimum for problem $(\mathcal{P}^+)$,

$$J^\star = \frac{1}{8\pi} \inf_{v \in C^+} J(v).$$

We denote $J^\star_{num}$ the corresponding value which was obtained numerically in the simulations above. The value $J^\star_{num}$ is represented as a function of Fr in Figure 9.

Estimate (3.5) shows that the theoretical value $J^\star$ must belong to the interval $[1, 2]$. This is verified numerically with $J^\star_{num}$ for $Fr \geq 3$ in Figure 9 (hence the term "global minimizer" for the points on the blue curve). In agreement with Theorem 4.5, the value $J^\star_{num}$ tends to 1 as Fr becomes large.

For $Fr = 2.45$, an optimal domain was also numerically obtained (Figure 7, top), but with the value $J^\star_{num} = 2.25$ which is clearly greater than 2. This case cannot correspond to a global minimizer and it is most likely a local minimizer of the problem.

The points on the blue curve were obtained as follows. We first computed the optimal domain for $Fr = 3.50$ by choosing a half disc as an initial guess for the minimization algorithm. We obtained the value $J^\star_{num} = 1.64$. The converged domain

was then used as an initial guess for the nearest Froude numbers on the blue curve ($Fr = 2.80$ and $Fr = 3.85$), and so on. For $Fr = 2.09$, the algorithm did not converge and a sinking phenomen was observed. Accordingly, we set $J^\star_{num} = 2$ for $Fr = 2.09$ in the Figure.

The sinking phenomenon was also numerically confirmed for the values $Fr = 1$, 1.25, 1.5 and 1.75 with a half disc as initial guess.

For $Fr \in (0.5, 1)$, the situation is completely different. We obtain an optimal domain which *cannot be a global minimizer* since the value $J^\star_{num}$ is a lot greater than 2. This value increases up to 10 for Fr close to 1. We obtain a domain which is numerically stable, so that it is likely to be a *local minimizer* for the problem. This reminds what happens for the Dirichlet energy with source term in a exterior domain in [21]: the global infimum is reached by a sequence of domains which "goes to infinity", whereas the most interesting cases are the local minimizers.

The points on the red curve were obtained as follows. We first computed the optimal domain for $Fr = 0.67$ with a half ellipse as initial guess for the minimization algorithm, namely $\{(x, z) \in \mathbb{R} \times (-\infty, 0],\ (x/1.1)^2 + (z/0.3)^2 \leq 1\}$. Then, the converged domain for $Fr = 0.67$ was used as initial guess for the closest Froude numbers on the red curve, and so on. The last point on the right of the red curve corresponds to a domain for which the algorithm did not clearly converge due to oscillations (hence the term "unstable" for this value).

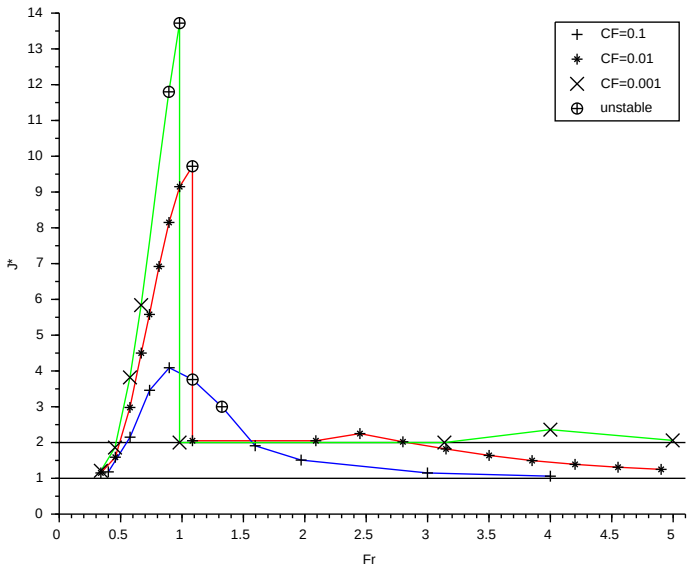

FIGURE 10. $J^\star$ vs Fr for three different drag coefficients

6.3. **Influence of the drag coefficient.** In all the previous simulations, the drag coefficient was equal to $C_F = 0.01$. We performed similar numerical simulations for $C_F = 0.1$ and $C_F = 0.001$, and we obtained comparable results. They are presented in Figure 10, where the value $J^\star_{num}$ is represented as a function of Fr.

The red curve in Figure 10 is the case $C_F = 0.01$ (cf. Figure 9). The horizontal line at the energy level 2 is the sinking phenomenon. For $C_F = 0.001$ (green curve) the importance of the normalized wave resistance functional J_{wave} is ten times greater than in the case $C_F = 0.01$. We recover the three previous situations, but the total resistance is higher. The sinking phenomenon happens on a larger interval of Froude numbers, typically between 1 and 3.

For $C_F = 0.1$ (blue curve) the normalized wave resistance is ten times smaller than in the model case $C_F = 0.01$. There is no sinking case here, but we still have the local minimizer for $Fr < 1$. The global minimizer happens for smaller Froude numbers, namely $Fr > 1.7$.

Acknowledgements

The authors are thankful to Leo Lazauskas for stimulating questions. The authors also acknowledge the group "Phydromat" for interesting discussions.

References

[1] G. Allaire. *Conception optimale de structures*, volume 58 of *Mathématiques & Applications*. Springer-Verlag, Berlin, 2007.

[2] G. P. Benham, J. P. Boucher, R. Labb, M. Benzaquen, and C. Clanet. Wave drag on asymmetric bodies. *Journal of Fluid Mechanics*, 878:147–168, 2019.

[3] L. Birk. *Fundamentals of Ship Hydrodynamics: Fluid Mechanics, Ship Resistance and Propulsion*. Wiley, 2019.

[4] J.-P. Boucher, R. Labbé, C. Clanet, and M. Benzaquen. Thin or bulky: Optimal aspect ratios for ship hulls. *Phys. Rev. Fluids*, 3:074802, Jul 2018.

[5] A. Braides. Γ-*convergence for beginners*, volume 22 of *Oxford Lecture Series in Mathematics and its Applications*. Oxford University Press, Oxford, 2002.

[6] L. Brasco, G. De Philippis, and B. Velichkov. Faber-Krahn inequalities in sharp quantitative form. *Duke Math. J.*, 164(9):1777–1831, 2015.

[7] H. Brezis. *Analyse fonctionnelle*. Collection Mathématiques Appliquées pour la Maîtrise. Masson, Paris, 1983.

[8] D. Bucur and G. Buttazzo. *Variational methods in shape optimization problems*. Progress in Nonlinear Differential Equations and their Applications, 65. Birkhäuser Boston, Inc., Boston, MA, 2005.

[9] G. Buttazzo. A survey on the Newton problem of optimal profiles. In *Variational analysis and aerospace engineering*, volume 33 of *Springer Optim. Appl.*, pages 33–48. Springer, New York, 2009.

[10] G. Buttazzo and B. Kawohl. On Newton's problem of minimal resistance. *Math. Intelligencer*, 15(4):7–12, 1993.

[11] S. M. Calisal, O. Goren, and D. B. Danisman. Resistance reduction by increased beam for displacement type ships. *J. Ship. Res.*, 3(46):208–213, 2002.

[12] J. Dambrine, E. Noviani, and Mo. Pierre. Rankine-type cylinders having zero wave resistance in infinitely deep flows. *IMA J. Appl. Math.*, 85(3):343–364, June 2020.

[13] J. Dambrine and Mo. Pierre. Regularity of optimal ship forms based on Michell's wave resistance. *Appl. Math. Optim.*, 2018.

[14] J. Dambrine, Mo. Pierre, and G. Rousseaux. A theoretical and numerical determination of optimal ship forms based on Michell's wave resistance. *ESAIM Control Optim. Calc. Var.*, 22(1):88–111, 2016.

[15] L. D. Ferreiro. The social history of the bulbous bow. *Technology and Culture*, 52(2):335–359, 2011.

[16] D. Gilbarg and N. S. Trudinger. *Elliptic partial differential equations of second order*. Classics in Mathematics. Springer-Verlag, Berlin, 2001.

[17] O. Goren, S.M. Calisal, and D. B. Danisman. Mathematical programming basis for ship resistance reduction through the optimization of design waterline. *J. Mar. Sci. Technol.*, 22:772–783, 2017.
[18] A. Sh. Gotman. The comperative criterion in deciding on the ship hull form with least wave resistance. In *Proceedings Colloquium EUROMECH 374*, pages 277–284, Poitiers, 1998.
[19] A. Sh. Gotman. Study of Michell's integral and influence of viscosity and ship hull form on wave resistance. *Oceanic Engineering International*, 6:74–115, 2002.
[20] A. Sh. Gotman. Navigating the wake of past efforts. *Journal of Ocean Technology*, 2(1):74–96, 2007.
[21] A. Henrot and Mi. Pierre. About critical points of the energy in an electromagnetic shaping problem. In *Boundary control and boundary variation (Sophia-Antipolis, 1990)*, volume 178 of *Lect. Notes Control Inf. Sci.*, pages 238–252. Springer, Berlin, 1992.
[22] A. Henrot and Mi. Pierre. *Variation et optimisation de formes*, volume 48 of *Mathématiques & Applications*. Springer, Berlin, 2005.
[23] C.-C. Hsiung. Optimal ship forms for minimum wave resistance. *J. Ship Res.*, 25(2), 1981.
[24] C.-C. Hsiung and S. Dong. Optimal ship forms for minimum total resistance. *J. Ship Res.*, 28(3), 1984.
[25] A. A. Kostyukov. *Theory of ship waves and wave resistance*. Effective Communications Inc., Iowa City, Iowa, 1968.
[26] M. G. Krein and V. G. Sizov. On the form of a ship of minimum total resistance (in Russian). unpublished, 1960.
[27] Z. Lian-en. Optimal ship forms for minimal total resistance in shallow water. *Schriftenreihe Schiffbau*, 445:1–60, 1984.
[28] W. C. Lin, W. C. Webster, and J. V. Wehausen. Ships of minimum total resistance. Technical Report No. NA-63-7, Institute of Engineering Research, University of California at Berkeley, 1963.
[29] J. P. Michalski, A. Pramila, and S. Virtanen. Creation of ship body form with minimum theoretical resistance using finite element method. In *Numerical Techniques for Engineering Analysis and Design*, pages 263–270. Springer Netherlands, 1987.
[30] J. H. Michell. The wave resistance of a ship. *Phil. Mag.*, 5(45):106–123, 1898.
[31] F. C. Michelsen. *Wave resistance solution of Michell's integral for polynomial ship forms*. PhD thesis, University of Michigan, 1960.
[32] V. G. Sizov. The seminar on ship hydrodynamics, organized by Professor M. G. Krein. In *Differential operators and related topics, Vol. I (Odessa, 1997)*, volume 117 of *Oper. Theory Adv. Appl.*, pages 9–20. Birkhäuser, Basel, 2000.
[33] E. Tuck and L. Lazauskas. Drag on a ship and Michell's integral. In *Proceedings of the XXII International Congress of Theoretical and Applied Mechanics, Adelaide, Australia*, 2008.
[34] E. O. Tuck. The wave resistance formula of J. H. Michell (1898) and its significance to recent research in ship hydrodynamics. *J. Austral. Math. Soc. Ser. B*, 30(4):365–377, 1989.
[35] E. O. Tuck, D. C. Scullen, and L. Lazauskas. Ship-wave patterns in the spirit of Michell. In A. C. King and Y. D. Shikhmurzaev, editors, *IUTAM Symposium on Free Surface Flows. Fluid Mechanics and Its Applications*, volume 62. Springer, Dordrecht, 2001.
[36] J. V. Wehausen. The wave resistance of ships. volume 13 of *Advances in Applied Mechanics*, pages 93 – 245. Elsevier, 1973.